

1 **New evidence for the Holocene development of active talus-foot rock glaciers at**
2 **Øyberget, southern Norway**

3
4
5
6 Atle Nesje¹, John A. Matthews², Henriette Linge¹, Marie Bredal³, Peter Wilson⁴ and
7 Stefan Winkler⁵

8
9 ¹ Department of Earth Science, University of Bergen and Bjerknes Centre for Climate
10 Research, NO-5020, Bergen, Norway

11 ² Department of Geography, College of Science, Singleton Park, Swansea University,
12 Swansea SA2 8PP, Wales, UK

13 ³ Geohazard and Earth Observation, Norges Geologiske Undersøkelse, Leiv Erikssons
14 vei 39, 7040 Trondheim, Norway

15 ⁴ School of Geography and Environmental Sciences, Ulster University, Coleraine, Co
16 Londonderry, BT52 1SA. Northern Ireland, UK

17 ⁵ Department of Geography and Geology, Julius-Maximilians-University Würzburg,
18 Am Hubland, D-97074 Würzburg, Germany

19
20
21
22 **Abstract**

23
24 Synthetic aperture radar interferometry (InSAR) demonstrates that lobate, blocky
25 depositional landforms at Øyberget, located ~1000 m below the lower climatic limit
26 of discontinuous permafrost in Ottadalen, southern Norway, are active rock glaciers.
27 Five years of InSAR data for six lobes demonstrate average surface movement of 1.2-
28 22.0 mm/year with maximum rates of 17.5-55.6 mm/year. New Schmidt-hammer
29 exposure-age dating (SHD) of two proximal lobes reveals mid-Holocene ages ($7.6 \pm$
30 1.3 and 6.0 ± 1.2 ka), which contrast with the early-Holocene ages obtained
31 previously from distal lobes, and late-Holocene SHD ages presented here from two
32 adjacent talus slopes (2.3 ± 1.0 and 2.4 ± 1.0 ka). Although passive transport of
33 boulders on the surface of these small, slow-moving rock glaciers means that the
34 exposure ages are close minimum estimates of the time elapsed since lobe inception,
35 disturbance of boulders on fast-moving rock glaciers is a source of potentially serious
36 underestimates of rock-glacier age. Rock-glacier development at Øyberget began
37 shortly after local deglaciation around 10 ka and continued throughout the Holocene
38 in response to microclimatic undercooling within the coarse blocky surface layer of
39 the talus and rock-glacier lobes. Undercooling is inferred to produce a negative
40 thermal offset of ~ 7 °C, which would be sufficient to develop sporadic permafrost at
41 the site and also to delay fast thawing of rock glaciers in a warming climate. Our
42 results point to circumstances where rock glaciers may be poor indicators of regional
43 climate and of limited usefulness in palaeoclimatic reconstruction.

44
45
46 **Key words:** talus-derived rock glacier, rock-slope failure, permafrost, active and
47 relict landforms, SAR interferometry, Schmidt-hammer exposure-age dating, Norway

48
49
50 **Introduction**

51

52 The lobate rock glaciers in Øybergsturdi, located beneath the south-facing rock wall of
53 Øyberget, upper Ottadalen, southern Norway (Figs 1a and 1b) are of significance for
54 several reasons. First, rock glaciers are relatively rare in southern Norway. In their
55 inventory, Lilleøren and Etzelmüller (2011) recognize 241 rock glaciers in Norway, of
56 which just 35 (<10%) are located in the south of the country (not including those at
57 Øyberget).

58

59 Second, Ballantyne (2018, p. 316) has disputed the existence of rock glaciers
60 at Øyberget and regards them instead as rockslide runout deposits, as has been
61 proposed for most, if not all, supposed rock glaciers in the British Isles (Ballantyne et
62 al., 2009; Wilson, 2009; Jarman et al., 2013). If his interpretation is correct, there are
63 implications for the identification of rock glaciers in Scandinavia and elsewhere, not
64 only for the landforms at Øyberget.

65

66 Third, rock glaciers are generally considered to be reliable indicators of a
67 permafrost environment (Haeberli, 1985; Barsch, 1996; Haeberli et al., 2006;
68 Berthling, 2011; Lilleøren et al., 2012; Kääh, 2013; Ballantyne, 2018), yet those at
69 Øyberget occur at ~530 m above sea level, which is ~1000 m below the present
70 estimated lower altitudinal limit of discontinuous permafrost in this region of southern
71 Norway (Etzelmüller and Hagen, 2005; Lilleøren et al., 2012; Gislås et al., 2016).

72 The Øyberget rock glaciers must therefore be either relict, or active at an
73 exceptionally low altitude. The preferred conclusion from our previous exposure-age
74 dating studies at the site using both the Schmidt hammer (Matthews et al., 2013) and
75 cosmogenic nuclides (Linge et al., 2020) was that these rock glaciers formed and
76 became relict (inactive) in the early Holocene, shortly after regional deglaciation.

77

78 The aim of this short paper is to re-evaluate the status, development and
79 implications of the Øyberget rock glaciers in the light of new evidence. We apply
80 synthetic aperture radar interferometry (InSAR) from the Norwegian Geological
81 Survey database (<http://insar.ngu.no>), which demonstrates present-day rock-glacier
82 creep at the site, and effectively disproves both the 'rockslide' and 'relict' hypotheses.
83 This evidence is supported by further exposure-age dating with the Schmidt hammer
84 on proximal rock-glacier lobes and adjacent talus, which has yielded significantly
85 younger dates than the previously dated distal lobes. In combination, the new
86 evidence indicates rock-glacier development at Øyberget throughout the Holocene.
87 Our revised interpretation has important implications for understanding the climatic
88 significance of rock glaciers and for exposure-age dating in the rock-glacier context.

89

90

91 **Øyberget rock glaciers and the environmental context**

92

93 Rock-glaciers occur at ~500-560 m a.s.l. at the foot of extensive ~200-m high talus
94 slopes (gradient 32-36°) that lie beneath the ~400-m high south-facing rock wall of
95 Øyberget (Fig. 1a). The best developed landforms (numbered 1-3), which were
96 investigated and dated previously by Matthews et al. (2013) and Linge et al. (2020),
97 extend ~200 m from the foot of the talus and have the characteristic lobate shape of
98 talus-foot rock glaciers. These lobes have steep (up to 40 °) distal slopes that stand up
99 to 20 m above the surrounding terrain. The upper surfaces of the lobes undulate and
100 have a few transverse ridges (gradients <8°).

101
102
103
104
105
106
107
108
109
110
111
112
113
114
115
116
117
118
119
120
121
122
123
124
125
126
127
128
129
130
131
132
133
134
135
136
137
138
139
140
141
142
143
144
145
146
147
148
149
150

All upper surfaces are composed of openwork large boulders (typical long axes 1-3 m; maximum 7 m). Talus boulders are of a similar size. Abutting the foot of the talus, narrower ledge-like lobes occur which, in a few places, have unstable distal slopes that reveal finer sedimentary material beneath the openwork boulders (Fig. 1b). Recent quarrying has revealed similar fine sediment in the toe of lobe 1. Although the rock glaciers are surrounded by Scots pine (*Pinus sylvestris*) forest, only scattered stunted trees grow from crevices between the boulders on the upper surface of some of the lobes. Lichens are typically present on most boulders but mosses and heath plant species are confined to patches of very thin soil in small depressions on boulder surfaces. Almost all boulders are firmly wedged together in the landform and perched boulders are rarely present.

Rocks in the region are mainly Precambrian gneiss (Lutro and Tveten, 1996). The Øyberget rock wall and the boulders in the rock glaciers are banded gneiss with distinctive layers of pink potassium feldspar, grey biotite-mica, and white quartz-feldspar. Complex northward-dipping banding in the rock wall would be expected to be relatively stable in relation to major rock-slope failure while being susceptible to frost weathering and supplying rockfall debris to the talus slopes and hence the rock glaciers.

Climatic normal data (AD 1961-1990) from Gjeilo-i-Skjåk meteorological station (378 m a.s.l.; 20 km down valley), adjusted for an altitudinal lapse rate of 0.65°C per 100 m, indicate a mean annual air temperature at the rock-glacier site of +1.6 °C (Aune, 1993). The corresponding mean January and mean July temperatures are -10.2 °C and +12.9 °C, respectively. Mean annual precipitation from the Gjeilo station is 295 mm, with a July maximum (Førland, 1993), which reflects the strong rain-shadow effect in this area of inland southern Norway. Modelled snow-depth data for the same period (<http://www.senorge.no>) indicate a maximum snow depth of only 38 mm in March. Although the precipitation and snow depth values may be a little higher at the site of the rock glaciers, they remain extremely low. More detailed climatic information is tabulated in Matthews et al. (2013) and Linge et al. (2020), and is available from eKlima (<http://sharki.oslo.dnmi.no>).

Deglaciation at the site of the Øyberget rock glaciers occurred at a time of rapid ice-sheet downwastage in the early Holocene. Local evidence, based on ¹⁰Be surface-exposure ages from the summit of Øyberget and from the valley floor ~2.0 km up-valley from the rock glaciers (Fig. 1a) was presented and discussed in the regional context by Linge et al. (2020). Corrected ¹⁰Be mean age (analytic uncertainty ±2σ) of summit samples was 11.2 ± 0.8 ka and of valley-floor samples was 10.1 ± 0.8 ka. These results are consistent with cosmogenic dating within the broader region (Goehring et al., 2008; Marr et al., 2018, 2019; Andersen et al., 2019), and with large-scale but less precise estimates based on deglaciation modelling in Scandinavia (Hughes et al., 2016; Stroeven et al., 2016). They also justify the ~9.7 ka deglaciation age used previously by Matthews et al. (2013) for Schmidt-hammer exposure-age dating of the rock glaciers close to the valley floor.

Previous investigation of the Øyberget rock glaciers has focused on exposure-age dating of boulders sampled from the surfaces of lobes 1-3 (Fig. 1a and 1b). Based on samples of 150 boulders, Schmidt-hammer exposure-age dating yielded ages (±2σ)

151 of 10.3 ± 1.3 , 9.9 ± 1.4 , and 9.0 ± 1.7 ka, respectively (Matthews et al. 2013). Based
152 on ^{10}Be surface-exposure dates obtained from three boulders on lobe 2 and four
153 boulders on lobe 3, Linge et al. (2020) obtained corrected mean ages of 11.2 ± 1.4 and
154 11.1 ± 2.4 ka (analytical uncertainty $\pm 2\sigma$), respectively. Taking account of the
155 uncertainties, the two techniques have therefore produced consistent results. The
156 techniques estimate, in different ways, the lapse of time since the boulders were first
157 exposed to the atmosphere. Interpretation of the early-Holocene exposure ages in
158 relation to the formation and development of the rock glaciers is discussed below.

159

160

161 **New evidence**

162

163 *InSAR data*

164

165 New evidence based on synthetic aperture radar interferiometry (InSAR) has recently
166 become available from the Norwegian Geological Survey database
167 (<http://insar.ngu.no>). InSAR Norge measures deformation of the Earth's surface as
168 one-dimensional velocities along the line-of-sight from satellite sensor to ground
169 surface. These data are particularly appropriate for exposed rock surfaces and are
170 particularly sensitive to vertical movements. Measurements are made from early June
171 to late September to avoid snow-cover effects. Data are available for particular points,
172 which are displayed on maps at variable scales, and groups of points can be selected
173 to define the average movement of specified areas of terrain, such as rock-glacier
174 surfaces. Time series of individual points and groups of points can also be analysed
175 and visualised graphically. Temporal coherence, for which a value of zero equals pure
176 noise and a value of 100 % is noise free, provides a measure of the reliability of data
177 points.

178

179 Mean velocity is negative (indicating reduced elevation and downslope
180 movement) for almost all measurement points on the rock-glacier surfaces over the
181 last five years (2015-2019) (Fig. 1c). Over the same period, almost all points from the
182 surrounding terrain, including the talus slopes and the Øyberget rock wall, recorded
183 zero velocity. In order to eliminate anomalous points and obtain representative mean
184 values for lobe surfaces, mean velocity was calculated for large clusters of points
185 from the fastest moving areas of each of lobes 1, 1*, 2, 2*, 3, 3* and 4 (Table 1), as
186 exemplified for lobes 2, 2*, 3 and 3* in Fig. 2. Other clusters of points that exhibit
187 relatively low but significant negative velocity values (west of lobe 1, and both west
188 and east of lobe 2; Fig. 1c) appear to indicate incipient lobes.

189

190 Lobes 2, 2* and 3* are the most active with a representative velocity of -15 to
191 -22 mm/year, while lobe 3 (representative velocity -1.2 mm/year) shows one very
192 small area of activity. Lobes 1, 1* and 4 show intermediate levels of activity
193 (representative velocity -10 to -12 mm/year). Maximum velocity recorded over the
194 five-year period at individual points is considerably higher for all measured lobes,
195 ranging between -17.5 (L 1*) and -55.6 mm/year (L 3*). Considering the velocity of
196 distal (1-3) and proximal (1*-3*) lobes in their respective matched pairs, the latter are
197 moving consistently faster than the former. Movement values exhibit near-linear
198 trends through time, as exemplified in Figs 3a-d, with consistent patterns within and
199 between years and temporal coherence values of >70 % for all lobes (Table 1).

200

201 In summary, with the exception of L 3, representative InSAR surface
202 velocities of the rock glaciers lie between -10 and -22 mm/year with consistent rates
203 of movement over the five-year monitoring period. Some lobes are moving faster than
204 others.

205
206 ***Schmidt-hammer exposure-age dating (SHD)***

207
208 The second line of new evidence is from SHD applied to three rock-glacier lobes
209 (L1*, L2* and L3*) located between lobes L1, L2 and L3 and the adjacent talus
210 slopes (Figs 1 and 2). The measurement techniques and approach to age-calibration
211 followed those used previously by Matthews et al. (2013) to date lobes L1-L3. R-
212 values (rebound values) were obtained using ‘type-N’ mechanical Schmidt hammers
213 (Proceq, 2004) from 150 boulders from the distal (outer) part of the surface of each
214 lobe and from near the foot of each talus slope. Five impacts were made on different
215 points of each boulder resulting in a mean R-value based on 750 individual impacts
216 from each surface. Quartzitic veins, boulder edges and cracks, and wet, steeply
217 sloping and lichen-covered surfaces were avoided. As a precaution against instrument
218 deterioration during use, frequent tests were made on the manufacturer’s test anvil.
219 The age-calibration equation of Matthews et al. (2013), based on local control points,
220 was used to produce surface exposure-age estimates. Confidence intervals (C_c ; 95
221 %) are based on combining the error of the calibration curve (C_c) with the sampling
222 error (C_c), using the method developed by Matthews and Owen (2010), Matthews and
223 Winkler (2011), and Matthews and McEwen (2013).

224
225 Schmidt-hammer results obtained from two of the proximal lobes (L2* and
226 L3*) are mid-Holocene in age (7.6 ± 1.3 and 6.0 ± 1.2 ka, respectively) and are
227 significantly younger than the early-Holocene ages obtained from the distal lobes
228 (Table 2 and Fig. 4). Their R-value distributions are more platykurtic and L2* exhibits
229 bimodality (Fig. 5). These features indicate mixed-age populations of boulders that
230 differ from the near-normal, unimodal distributions of the distal lobes (particularly
231 L1) and, especially, the older control surface. The age obtained from L1* (11.3 ± 1.3
232 ka) is, however, significantly older than the other proximal lobes and comparable with
233 the ^{10}Be cosmogenic dates of 11.2 ± 1.4 and 11.1 ± 2.4 ka obtained by Linge et al.
234 (2020) for distal lobes L2 and L3, respectively.

235
236 Two of the talus slopes (T2 and T3) yielded late-Holocene ages (2.4 ± 1.0 and
237 2.3 ± 1.0 ka, respectively) that are significantly younger than those of any of the rock-
238 glacier lobes (Fig. 4). One talus site (T1) is significantly older than the other two talus
239 sites, and does not have the unimodal and leptokurtic distribution of either T2 and T3
240 or the younger control surface (Fig. 5). Again, this suggests T1 is characterised by a
241 mixed-age population of boulders. Thus, six of the Schmidt-hammer exposure ages
242 exhibit a remarkably consistent temporal pattern with underlying unimodal
243 distributions that are approximately normal and signify single-age populations.
244 Indeed, three pairs of sites (L2 and L3, L2* and L3*, and T2 and T3) have yielded
245 significantly different ages between pairs according to the confidence intervals,
246 whereas within-pair differences are not significantly different (Fig. 4). The common
247 characteristic of the three remaining ages that do not conform to this pattern (L1, L1*
248 and T1*) is that they have each yielded the oldest ages in their respective categories, a
249 possible explanation for which is a systematic difference in the stability of the
250 Øyberget rock wall towards its western end.

251

252

In summary, two of the three proximal rock-glacier lobes have yielded mid-Holocene SHD ages that are younger than the three previously-dated early-Holocene distal lobes. Two of the three talus-slope sites date from the late Holocene and are significantly younger than all the rock-glacier sites,

256

257

258 **Discussion**

259

260 *Active rock glaciers versus relict rock-slope failures*

261

Identification of rock glaciers and distinguishing them from rock-slope failures and other boulder-dominated landforms is a controversial interpretive problem in geomorphology. The problem arises from the possibility of similar morphologies arising from different formative processes; that is, it is an example of landform mimicry or equifinality (Haines-Young and Petch, 1983; Schumm, 1993; Bevan et al., 1996; Wilson, 2009; Knight et al., 2019). Rock glaciers and rock-slope failures are both coarse-debris deposits located at the foot of steep mountain slopes, which can appear remarkably similar in relation to size, surface features and composition.

270

271

Initial recognition of the Øyberget distal lobes as talus-foot rock glaciers was based on several morphological criteria (Matthews et al., 2013), including: (1) the lack of scars or indentations in the Øyberget rock wall that would indicate the source of large-scale rock-slope failures; (2) the relatively uniform boulder size pointing to the piecemeal addition of rockfall material rather than the failure of major sections of the rock wall; (3) the small scale of the lobes relative to the height of fall and hence potential run-out distance likely to be generated following failure of the rock wall; and (4) the integrity of the lobes, their steep distal slopes and transverse ridges, all of which are features consistent with rock-glacier creep. These criteria are not, however, definitive.

281

282

The same recognition/equifinality problem has been recently rehearsed in the British Isles where, after several decades of identifying relict rock glaciers (e.g. Dawson, 1977; Chattopadhyay, 1984; Wilson, 1990a, 1990b; Maclean, 1991) many have been re-interpreted as rock-slope failures and a consensus appears to have been reached that there are no *bona fide* rock glaciers (Wilson, 2004, 2009; Harrison et al., 2008; Ballantyne et al., 2009; Jarman et al., 2013). Instead, the landforms previously recognised as rock glaciers have been, almost without exception, firmly identified as rock-slope failures.

289

290

291

292

293

294

295

296

297

298

299

In contrast, there are numerous rock glaciers in Norway: of the 241 included in the inventory of Lilleøren and Etzelmüller (2011), most are talus-derived or talus-foot features. However, rock glaciers are uncommon in southern Norway, where only 23 talus-foot rock glaciers were recognised by Lilleøren and Etzelmüller (2011). Ballantyne (2018, p. 316) has claimed that the Øyberget rock glaciers are misinterpreted rockslides, and Wilson et al. (2020) have argued that a boulder-dominated landform assemblage in Alnesdalen, previously mapped as a rock glacier by Sollid and Kristiansen (1984), is mainly the product of one or more rock-slope failures (though attribution of part of this feature to a rock-glacier origin could not be

300 rejected). Apart from these two exceptions, the problem of differentiating rock
301 glaciers from rock-slope failures appears not to have been addressed in Norway.

302

303 At Øyberget, the InSAR evidence of movement (Table 1; Figures 1c and 2) is
304 unequivocal in demonstrating that the talus-foot lobes are currently active. As such we
305 consider them to be active rock glaciers rather than relict rock-slope failures.
306 Representative velocities of ~10-20 mm per year and the maximum velocity of ~50
307 mm per year are low in comparison to measured rates of creep of active rock glaciers
308 elsewhere, even for 'cold' polar rock glaciers (Kääb et al., 2002; Bollmann et al.,
309 2015; Ballantyne, 2018). Considerable variations in seasonal and annual rates of
310 movement of rock glaciers occur in response to climate, involving both the thermal
311 regime and precipitation (Kääb et al., 2007; Serrano et al., 2010; Cicoira et al., 2019).
312 It should not be assumed, therefore, that the movement rates derived from InSAR over
313 the five-year monitoring period are applicable to the past.

314

315 The sequential increase in exposure age from the talus slopes, through the
316 proximal lobes to the distal lobes is also convincing evidence against a rock-slope
317 failure origin for the Øyberget lobes. Several studies have demonstrated consistent
318 patterns of increasing SHD age of boulders down the axis of relatively long rock-
319 glacier tongues (Frauenfelder et al., 2005; Kellerer-Pirklbauer et al., 2008; Böhlert et
320 al., 2011; Rode and Kellerer-Pirklbauer, 2012; Winkler and Lambiel, 2018). Such
321 patterns are clearly inconsistent with the synchronous surface of deposits formed as a
322 result of rock-slope failure, the debris of which would be of uniform age. However,
323 previous exposure-age dating of the distal lobes yielded only early-Holocene ages
324 (Matthews et al., 2013; Linge et al., 2020). In the absence of dates from proximal
325 lobes and of InSAR data, this led to these authors' incorrect conclusion that the
326 Øyberget rock glaciers have synchronous surfaces and are relict.

327

328 *Formation and development of rock glaciers*

329

330 SHD provides estimates of the average exposure age of the boulders on the rock-
331 glacier surface. At least two generations of lobes are indicated from the SHD results
332 (Table 2 and Figure 4). First, the boulders on the surface of the distal lobes with
333 average ages of 9.0-10.3 ka must have been deposited on the rock-glacier surface in
334 the early Holocene and appear to have been transported passively with only minimal
335 disturbance since then. These inferences are supported by the results of ¹⁰Be
336 exposure-age dating of individual boulders from the same lobes (Linge et al., 2020).
337 Rates of movement of 10-20 mm per year from the InSAR data are sufficient,
338 moreover, to account for the development of small lobes of length 100-200 m over a
339 period of ~10 ka. Second, the exposure ages of ~6.0-7.6 ka obtained from two of the
340 proximal lobes indicate somewhat later development, which is compatible with the
341 faster InSAR velocities recorded from these lobes (especially the fastest moving lobe
342 L3*).

343

344 Exposure-ages of 2.3-9.0 ka obtained from the talus slopes indicate that
345 whereas some of the talus is much younger than the rock-glacier lobes (and remains
346 active today), other parts date from the early Holocene and are of comparable age to
347 the lobes. The scale of the talus slopes suggests, moreover, that much of the talus
348 volume is likely to have accumulated in the early Holocene when, shortly after
349 deglaciation at ~10 ka, boulder supply from the Øyberget rock wall initiated distal

350 lobe formation. Development of the lobes may therefore have benefited from
351 enhanced (paraglacial) debris inputs from the rock wall following glacial unloading
352 and debulking (cf. Cossart et al., 2008; McColl, 2012; Ballantyne et al., 2014;
353 Deline et al., 2015).

354
355 The development of the rock-glacier lobes requires not only sufficient debris
356 supply but also cohesive flow of perennially frozen ice-rock mixtures (permafrost
357 creep). This, in turn requires reduction of internal friction and the build-up of
358 cohesion within the talus by excess ice (ice supersaturation) beyond the pore space of
359 the rock particles (Haeberli et al., 2006). On account of the relatively low altitude
360 (~530 m a.s.l.) of the Øyberget lobes, *regional* climatic conditions today are not
361 conducive to permafrost development. The present lower limit of discontinuous
362 permafrost in this region of southern Norway is estimated to lie at ~1500 m a.s.l.
363 (Etzelmüller and Hagen, 2005; Gisnås et al., 2016), probably higher at this south-
364 facing locality. In addition, such regional permafrost limits are unlikely to have been
365 greater than a few hundred metres lower than at present at any time during the
366 Holocene (Lilleøren et al., 2012). The presence of rock-glaciers in such an apparently
367 inauspicious location therefore requires suitable *local* environmental conditions for
368 development of (1) a persistent subsurface permafrost thermal regime and (2)
369 sufficient excess ice within the sedimentary voids.

370
371 There have been notable observations of permafrost in coarse blocky
372 openwork deposits such as blockfields, talus and rock glaciers, where mean air
373 temperatures appear too high for its development (Juliussen and Humlum, 2008;
374 Sawada et al., 2003; Stiegler et al., 2014; Morard et al., 2010; Popescu et al., 2017).
375 Indeed, Zacharda et al. (2007) have reported patchy permafrost-like conditions in
376 central European talus where the mean annual air temperature is 6.8–7.5 °C. A
377 negative thermal offset of this scale is sufficient to account for the presence of
378 permafrost in the talus-foot rock glaciers ~1000 m below the lower altitudinal limit of
379 discontinuous permafrost at Øyberget.

380
381 Various microclimatic mechanisms have been proposed to explain the thermal
382 offset associated with the coarse surface layer of rock glaciers with or without a
383 winter snow cover (Ballantyne, 2018; Jones et al., 2019; Wagner et al., 2019; Wicky
384 and Hauck, 2020). The mechanisms involve heat exchange by advection and/or
385 convection in the interconnected void spaces between boulders, conduction through
386 the boulders themselves, or thermal radiation. The most cited mechanisms, which
387 include ‘Balch ventilation’ (Balch, 1900; Humlum, 1997; Harris and Pedersen, 1998)
388 and the ‘chimney effect’ (Hanson and Hoelzle, 2004; Delaloye and Lambiel, 2005;
389 Kellerer-Pirklbauer et al., 2015), involve cold, dense air displacing warmer air from
390 the void space in winter. We propose that one or more of these mechanisms promote
391 and maintain a subsurface permafrost thermal regime within the Øyberget rock
392 glaciers, assisted by the very low air temperatures and thin snow cover. In effect, the
393 cold winters in this region of southern Norway compensate for quite extreme summer
394 warmth.

395
396 Groundwater, rain and snow meltwater are possible sources of liquid water
397 necessary for excess ice development within the Øyberget rock-glacier lobes under a
398 negative mean annual ground temperature regime (cf. Haeberli and Vonder Mühll,
399 1996). Rain from the summer and autumn rainfall maximum, and meltwater from

400 winter snowfall, including snow deposited on the talus slopes from snow-avalanches
401 (cf. Humlum et al., 2007), are likely to be the most important sources. However, no
402 observations or geophysical evidence relating to the nature of the ice within the
403 Øyberget lobes are available. The hypothesis favoured previously that, following
404 deglaciation, residual glacier ice may have been buried by paraglacial debris
405 accumulation at the base of the Øyberget rock wall, and that this may have triggered
406 rock-glacier formation (Matthews et al., 2013; Linge et al., 2020), is considered
407 unnecessary. Thus, the new evidence presented in this paper has led to what is
408 essentially a microclimatic hypothesis for rock-glacier inception in the early Holocene
409 with development continuing throughout the Holocene to the present day.

410

411 *Climatic and dating implications of rock glaciers*

412

413 Our results from Øyberget demonstrate that active rock glaciers can occur well
414 beyond supposed regional climatic limits owing to the development of
415 microclimatically-induced permafrost. The occurrence of sporadic permafrost at
416 ~1000 m below the lower altitudinal limit of discontinuous permafrost is equivalent to
417 a negative thermal offset of at least ~7 °C. This exposes the limitations on using the
418 distribution of active rock glaciers as climatic indicators, and relict rock glaciers in
419 palaeoclimatic reconstruction (cf. Humlum, 1998). Although not presenting a major
420 problem in areas where rock glaciers are common, and anomalies can be readily
421 identified, azonal cases could be of major importance in regions, like southern
422 Norway, where environments are marginal for rock glaciers. In the context of a
423 warming climate, the same microclimatic processes that create undercooling and
424 enable permafrost development beneath the coarse surface layer of rock glaciers,
425 should render rock glaciers resilient and preserve them from fast thawing during the
426 transition from active to relict (cf. Jones et al., 2019; Wagner et al., 2019).

427

428 We have also demonstrated that relatively old exposure ages of boulders on
429 rock glaciers may suggest relict status when in fact the rock glaciers are still active
430 due to largely passive transport of the surface boulders. In general, the exposure age
431 of surface boulders from distal parts of rock glaciers provide minimum estimates of
432 the time elapsed since the boulders were first exposed to the atmosphere. If the rock
433 glacier is small and slow moving (or was slow moving in the case of a relict rock
434 glacier), then boulders are likely to have been little disturbed during transport on the
435 rock glacier surface and hence their exposure age may be a close approximation to
436 rock-glacier age in the sense of the time elapsed since formation began (rock-glacier
437 inception). This is the situation in the case of the rock-glacier lobes at Øyberget,
438 which date from various times within the early and mid Holocene. However, the faster
439 a rock glacier moves the more likely that the boulders will be disturbed during
440 transport, and the greater the likelihood that the exposure age will deviate from the
441 age of the landform. High rates of boulder turnover during transport may lead to gross
442 underestimates of landform age. Once fast-moving rock glaciers with high boulder
443 turnover become relict (cease to move) exposure ages may approximate the lapse of
444 time since stabilisation, rather than landform age.

445

446

447 **Conclusion**

448

449 New evidence from the Øyberget landforms has necessitated re-evaluation of the
450 previous interpretations of Matthews et al. (2013) and Linge et al. (2020) in relation to
451 their nature, status, age, development and implications, and has led to the following
452 conclusions:

453

454 (1) The talus-foot lobes are correctly interpreted as rock glaciers: they are not relict
455 rock-slope failures.

456

457 (2) InSAR data demonstrate that the rock glaciers are active today with representative
458 surface velocities from six lobes (AD 2015-2019) ranging from 1.2-22.0 mm/year and
459 maximum velocities of 17.5-55.6 mm/year.

460

461 (3) SHD demonstrates that two of three proximal lobes are of mid-Holocene age (7.6
462 ± 1.3 and 6.0 ± 1.2 ka) and two of three adjacent areas of talus are of late-Holocene
463 age (2.3 ± 1.0 and 2.4 ± 1.0 ka). The new results are significantly younger than the
464 previously published SHD and ^{10}Be exposure ages from three distal lobes that indicate
465 early-Holocene ages (up to 11.2 ± 1.4 ka).

466

467 (4) Passive transport of boulders on the surface of these small, slowly-moving rock
468 glaciers produces exposure ages that represent close minimum estimates of the time
469 elapsed since rock glacier inception. In contrast, on rapidly-moving rock glaciers,
470 such exposure ages may be gross underestimates of the rock-glacier age due to high
471 rates of boulder disturbance and turnover.

472

473 (5) Following (paraglacial) inception of rock-glacier formation shortly after retreat of
474 the Scandinavian Ice Sheet from the site around 10 ka, the evidence indicates that at
475 least two generations of rock-glacier development have occurred during the Holocene.

476

477 (6) Development of permafrost at the site, ~ 1000 m below the present lower climatic
478 limit of discontinuous permafrost, suggests that microclimatic undercooling within the
479 coarse blocky surface layer of the talus and rock-glacier lobes is responsible for a
480 negative thermal offset of at least 7.0 °C. This enables growth in the void space of the
481 excess ice necessary for rock-glacier creep and preserves rock glaciers from fast
482 thawing in a warming climate.

483


484 (7) However, undercooling may limit the value of rock glaciers as indicators of
485 regional climate, and hence limit their use for palaeoclimatic reconstruction,
486 especially in regions that are marginal for rock-glacier development.

487

488

489 **Acknowledgements**

490

491 We thank Professor W. Haeberli for his informal comments on our previous
492 interpretations of the Øyberget rock glaciers, some of which we have taken the
493 opportunity to correct in this paper. Thanks are also due to Anna Ratcliffe for
494 preparing the figures for publication. This paper represents Jotunheimen Research
495 Expeditions Contribution No.  (see <http://jotunheimenresearch.wixsite.com/home>).

496

497

498 **References**

499
500 Andersen JL, Egholm DL, Knudsen MF, Linge H, Jansen JD, Goodfellow BW,
501 Pedersen VK, Tikhomirov D, Olsen J, Fredin O (2019) Pleistocene evolution of a
502 Scandinavian plateau landscape. *Journal of Geophysical Research: Earth Surface*
503 123, doi.org/10.1029/2018JF004670.
504
505 Aune B (1993) *Temperaturnormaler: Normalperiode 1961–90*. Det Norske
506 Meteorologiske Institutt: Oslo.
507
508 Balch ES (1900) *Glacières; or, Freezing Caverns*. Allen, Lane and Scott: Philadelphia.
509
510 Ballantyne CK (2018) *Periglacial Geomorphology*. Wiley: Chichester.
511
512 Ballantyne CK, Schnabel C, Xu S (2009) Exposure dating and reinterpretation of
513 coarse debris accumulations ('rock glaciers') in the Cairngorm Mountains, Scotland.
514 *Journal of Quaternary Science* 24, 19-31.
515
516 Ballantyne CK, Wilson P, Gheorghiu D, Rodés À (2014) Enhanced rock-slope failure
517 following ice-sheet deglaciation: timing and causes. *Earth Surface Processes and*
518 *Landforms* 39, 900-913.
519
520 Barsch D (1996) *Rock Glaciers: Indicators for the Present and Former Geoecology of*
521 *High Mountain Environments*. Springer-Verlag: Berlin.
522
523 Berthling I (2011) Beyond confusion: rock glaciers as cryo-conditioned landforms.
524 *Geomorphology* 131: 98-106.
525
526 Bevan K (1996) Equifinality and uncertainty in geomorphological modelling. In
527 Rhodes BL, Thorn CE (eds). *The Scientific Nature of Geomorphology*. Wiley:
528 Chichester, 289-313.
529
530 Böhlert R, Compeer M, Egli M, Brandova D, Maisch M, Kubik PW, Haeberli W
531 (2011) A combination of relative-numerical dating methods indicates two high Alpine
532 rock glacier activity phases after the glacier advance of the Younger Dryas. *The Open*
533 *Geography Journal* 4, 115-130.
534
535 Bollmann E, Girstmair A, Mitterer S (2015) A rock glacier activity index based on
536 rock glacier thickness changes and displacement rates inferred from airborne laser
537 scanning. *Permafrost and Periglacial Processes* 26, 347-359.
538
539 Chattopadhyay GP (1984) A fossil valley-wall rock glacier in the Cairngorm
540 Mountains. *Scottish Journal of Geology* 20, 121-125.
541
542 Cicoira A, Beutel J, Faillettaz J, Vieli A (2019) Water controls the seasonal rhythm of
543 rock glacier flow. *Earth and Planetary Science Letters* 528, 115844.
544
545 Cossart E, Braucher R, Fort M, Bourlés DL, Carcaillet J (2008) Slope instability in
546 relation to glacial debuttressing in alpine areas (upper Durance catchment,
547 southeastern France): evidence from field data and ¹⁰Be cosmic ray exposure ages.
548 *Geomorphology* 95, 3-26.

549
550 Delaloye R, Lambiel C (2005) Evidence of winter ascending air circulation
551 throughout talus slopes and rock glaciers situated in the lower belt of alpine
552 discontinuous permafrost. *Norsk Geografisk Tidsskrift/Norwegian Journal of*
553 *Geography* 59: 194-203.
554
555 Deline P, Gruber S, Delaloye R, Fischer L, Geertseema M, Giardino M, Hasler A,
556 Kirkbride M, Krautblatter M, Magnin F (2015) Ice loss and slope stability in high-
557 mountain regions. In Haeberli W, Whitman C (eds.) *Snow and Ice-related Hazards,*
558 *Risks and Disasters*. Amsterdam: Elsevier, 521-561.
559
560 Dawson AG (1977) A fossil lobate rock glacier in Jura. *Scottish Journal of Geology*
561 13, 31-42.
562
563 Etzelmüller B, Hagen JO (2005) Glacier-permafrost interaction in Arctic and alpine
564 mountain environments with examples from southern Norway and Svalbard. In Harris
565 C, Murton JB (eds) *Cryospheric Systems: Glaciers and Permafrost*. Geological
566 Society, London, Special Publication 242, 11-27.
567
568 Førland EJ (1993) *Nedbørnormaler: Normalperiode 1961–90*. Det Norske
569 Meteorologiske Institutt: Oslo.
570
571 Frauenfelder R, Laustela M, Kääh A (2005) Relative-age dating of Alpine rockglacier
572 surfaces. *Zeitschrift für Geomorphologie NF* 49, 145-166.
573
574 Gislås K, Etzelmüller B, Lussana C, Hjort J, Sannel ABK, Isaksen K, Westermann S,
575 Kuhry P, Christiansen H, Frampton A, Åkerman J (2017) Permafrost map for
576 Norway, Sweden and Finland. *Permafrost and Periglacial Processes* 28, 359-378.
577
578 Goehring BM, Brook EJ, Linge H, Raisbeck GM, Yiou F (2008) Beryllium-10
579 exposure ages of erratic boulders in southern Norway and implications for the history
580 of the Fennoscandian Ice Sheet. *Quaternary Science Reviews* 27, 320-336.
581
582 Haeberli W (1985) Creep of mountain permafrost: internal structure and flow of
583 Alpine rock glaciers. *Mitteilungen der Versuchsanstalt für Wasserbau, Hydrologie*
584 *and Glaziologie* 77, 1-142.
585
586 Haeberli W, Vonder Mühl D (1996) On the characteristics and possible origins of ice
587 in rock glacier permafrost. *Zeitschrift für Geomorphologie Supplement Band* 49, 145-
588 166.
589
590 Haeberli W, Hallet B, Arenson L, Elconin R, Humlum O, Kääh A, Kaufmann V,
591 Ladanyi B, Matsuoka N, Springman S, Vonder Mühl D (2006) Permafrost creep and
592 rock glacier dynamics. *Permafrost and Periglacial Processes* 17, 189-214.
593
594 Haines-Young RH, Petch JR (1983) Multiple working hypotheses: equifinality and
595 the study of landforms. *Transactions of the Institute of British Geographers NS* 8,
596 458-466.
597

598 Hanson S, Hoelzle M (2004) The thermal regime of the active layer at the Murtèl rock
599 glacier based on data from 2002. *Permafrost and Periglacial Processes* 15, 273-282.
600

601 Harris SA, Pedersen DE (1998) Thermal regimes beneath coarse blocky material.
602 *Permafrost and Periglacial Processes* 9, 107-120.
603

604 Harrison S, Whalley B, Anderson E (2008) Relict rock glaciers and protalus lobes in
605 the British Isles: implications for Late Pleistocene mountain geomorphology and
606 palaeoclimate. *Journal of Quaternary Science* 23, 287-304.
607

608 Hughes ALC, Gyllencreutz R, Lohne Ø, Mangerud J, Svendsen JL (2016) The last
609 Eurasian ice sheets – a chronological database and time-slice reconstruction, DATED-
610 1. *Boreas* 45, 1-45.
611

612 Humlum O (1997) Active layer thermal regime at three rock glaciers in Greenland.
613 *Permafrost and Periglacial Processes* 8, 383-408.
614

615 Humlum O (1998) The climatic significance of rock glaciers. *Permafrost and*
616 *Periglacial Processes* 9, 375-395.
617

618 Humlum O, Christiansen HH, Juliussen H (2007) Avalanche-derived rock glaciers in
619 Svalbard. *Permafrost and Periglacial Processes* 18, 75-88.
620

621 Jarman D, Wilson P, Harrison S (2013) Are there any rock glaciers in the British
622 mountains. *Journal of Quaternary Science* 28, 131-143.
623

624 Jones DB, Harrison S, Anderson K, Whalley WB (2019) Rock glaciers and mountain
625 hydrology: a review. *Earth-Science Reviews* 193: 66-90.
626

627 Juliussen H, Humlum O (2008) Thermal regime of openwork block fields on the
628 mountains Elgåhogna and Sølen, central-eastern Norway. *Permafrost and Periglacial*
629 *Processes* 19: 1-18.
630

631 Käab A (2013) Rock glaciers and protalus forms. In Elias SA (ed) *Encyclopedia of*
632 *Quaternary Science, volume 3, 2nd edition*. Elsevier: Amsterdam, 535-552.
633

634 Käab A, Isaksen K, Eiken T, Farbrot H (2002) Geometry and dynamics of two lobe-
635 shaped rock glaciers in the permafrost of Svalbard. *Norsk Geografisk*.
636 *Tidsskrift/Norwegian Journal of Geography* 56, 152-160.
637

638 Käab A, Frauenfelder R, Roer I (2007) On the response of rock glacier creep to
639 surface temperature increase. *Global and Planetary Change* 56, 172-187.
640

641 Kellerer-Pirklbauer A, Wangenstein B, Farbrot H, Etzelmüller B (2008) Relative
642 surface age-dating of rock glacier systems near Hólar in Hjaltadalur, northern Iceland.
643 *Journal of Quaternary Science* 23, 137-151.
644

645 Kellerer-Pirklbauer A, Pauritsch M, Winkler G (2015) Widespread occurrence of
646 ephemeral funnel hoarfrost and related air ventilation in coarse-grained sediments of a

647 relict rock glacier in the Seckauer Tauern Range, Austria. *Geografiska Annaler Series*
648 *A (Physical Geography)* 97, 453-471.

649

650 Knight J, Harrison S, Jones DB (2019) Rock glaciers and the geomorphological
651 evolution of deglaciating mountains. *Geomorphology* 324, 14-24.

652

653 Lilleøren KS, Etzelmüller B (2011) A regional inventory of rock glaciers and ice-
654 cored moraines in Norway. *Geografiska Annaler Series A (Physical Geography)* 93,
655 175-191.

656

657 Lilleøren KS, Etzelmüller B, Schuler TV, Gisnås K, Humlum O (2012) The relative
658 age of mountain permafrost – estimation of Holocene permafrost limits in Norway.
659 *Global and Planetary Change* 92-93, 209-223.

660

661 Linge H, Nesje A, Matthews JA, Fabel D, Xu S (2020) Evidence for rapid paraglacial
662 formation of rock glaciers in southern Norway from ¹⁰Be surface-exposure dating.
663 *Quaternary Research* 97, 55-70.

664

665 Lutro O, Tveten E (1996) *Geologisk kart over Norge, bergrunnskart Årdal M*
666 *1:250,000*. Norges Geologiske Undersøkelse: Trondheim.

667

668 Maclean AF (1991) *The formation of valley-wall rock glaciers*. PhD thesis, University
669 of St. Andrews.

670

671 Marr P, Winkler S, Löffler J (2018) Investigations on blockfields and related
672 landforms at Blåhø (Southern Norway) using Schmidt-hammer exposure-age dating:
673 palaeoclimatic and morphodynamic implications. *Geografiska Annaler Series A*
674 *(Physical Geography)* 100, 285-306.

675

676 Marr P, Winkler S, Binnie SA, Löffler J (2019) ¹⁰Be-based exploration of the timing
677 of deglaciation in two selected areas of southern Norway. *E&G Quaternary Science*
678 *Journal* 68, 165-176.

679

680 Matthews JA, McEwen LJ (2013) High-precision Schmidt-hammer exposure-age
681 dating (SHD) of flood berms, Vetlestølsdalen, alpine southern Norway: first
682 application and some methodological issues. *Geografiska Annaler, Series A (Physical*
683 *Geography)* 95, 185-195.

684

685 Matthews JA, Owen G (2010) Schmidt-hammer exposure-age dating: developing
686 linear age-calibration curves using Holocene bedrock surfaces from the Jotunheimen-
687 Jostedalbreen regions of southern Norway. *Boreas* 39, 105-115.

688

689 Matthews JA, Winkler S (2011) Schmidt-hammer exposure-age dating (SHD):
690 application to early Holocene moraines and a reappraisal of the reliability of terrestrial
691 cosmogenic nuclide dating (TCND) at Austanbotnbreen, Jotunheimen, Norway.
692 *Boreas* 40, 256-270.

693

694 Matthews JA, Nesje A, Linge H (2013) Relict talus-foot rock glaciers at Øyberget,
695 upper Ottadalen, southern Norway. *Permafrost and Periglacial Processes* 24, 336-
696 346.

697
698 McColl ST (2012) Paraglacial rock-slope stability. *Geomorphology* 153-154, 1-16.
699
700 Morard S, Delaloye R, Lambiel C (2010) Pluriannual thermal behaviour of low
701 elevation cold talus slopes in western Switzerland. *Geographica Helvetica* 65, 124-
702 134.
703
704 Popescu R, Vespremeanu-Stroe A, Onaca A, Vasile M, Cruceru N, Pop O (2017)
705 Low-altitude permafrost research in an overcooled talus slope-rock glacier system in
706 the Romanian Carpathians (Detunata Goală, Apuseni Mountains). *Geomorphology*
707 295, 840-854.
708
709 Proceq (2004) *Operating instructions. Betonprüfhammer N/NR-L/LR*. Proceq SA:
710 Schwerzenbach.
711
712 Rode M, Kellerer-Pirklbauer A (2012) Schmidt-hammer exposure-age dating (SHD)
713 of rock glaciers in the Schöderkogel-Eisenhut area, Schladminger Tauern Range,
714 Austria. *The Holocene* 22, 761-771.
715
716 Sawada Y, Ishikawa M, Ono Y (2003) Thermal regime of sporadic permafrost on a
717 block slope on Mt Nishi-Nupukasushinupuri, Hokkaido Island, northern Japan.
718 *Geomorphology* 52, 121-130.
719
720 Schumm SA (1993) *To Interpret the Earth – Ten Ways to be Wrong*. Cambridge
721 University Press: Cambridge.
722
723 Serrano E, de SanjoséJJ, González-Trueba JJ (2010) Rock glacier dynamics in
724 marginal periglacial environments. *Earth Surface Processes and Landforms* 35, 1302-
725 1314.
726
727 Sollid JL, Kristiansen K (1984) *Raumavassdraget, Kvartaergeologi og geomorfologi,*
728 *I: 80,000*. Universitetet I Oslo, Geografisk Institutt.
729
730 Stiegler C, Rode M, Sass O, Otto JC (2014) An undercooled scree slope detected by
731 geophysical investigations in sporadic permafrost below 1000 m asl, central Austria.
732 *Permafrost and Periglacial Processes* 25, 194-207.
733
734 Stroeven AP, Hätestrand C, Kleman J, Heyman J, Fabel D, Fredin O, Goodfellow W,
735 Harbor JM, Jansen JD, Olsen L, Caffee MW, Fink D, Lundqvist J, Rosqvist GC,
736 Strömberg B, Jansson KN (2016) Deglaciation of Fennoscandia. *Quaternary Science*
737 *Reviews* 147, 91-121.
738
739 Wagner T, Pauritsch M, Mayaud C, Kellerer-Pirklbauer A, Thalheim F, Winkler G
740 (2019) Controlling factors of microclimate in blocky surface layers of two nearby
741 relict rock glaciers (Niedere Tauern Range, Austria). *Geografiska Annaler, Series A*
742 *(Physical Geography)* 101, 310-333.
743
744 Walker M, Head MJ, Berkelhammer M, Björk S, Cheng H, Cwynar L, Fisher D,
745 Gkinis V, Long A, Lowe J, Newnham R, Rasmussen SO, Weiss H (2018) Formal
746 ratification of the subdivision of the Holocene Series/Epoch (Quaternary

747 System/Period): two new Global Boundary Stratotype Sections and Points (GSSPs)
748 and three new stages/subseries. *Episodes* 41(4), 1-11.
749 DOI:10.18814/episodes/2018/018016.
750

751 Wicky J, Hauck C (2020) Air convection in the active layer of rock glaciers. *Frontiers*
752 *in Earth Science* 8, 335. DOI:10.3389/feart.2020.00335.
753

754 Wilson P (1990a) Characteristics and significance of proglacial ramparts and fossil rock
755 glaciers on Errigal Mountain, County Donegal. *Proceedings of the Royal Irish*
756 *Academy* 90B, 1-21.
757

758 Wilson P (1990b) Morphology, sedimentological characteristics and origin of a fossil
759 rock glacier on Muckish Mountain, County Donegal, northwest Ireland. *Geografiska*
760 *Annaler Series A (Physical Geography)* 72A, 237-247.
761

762 Wilson P (2004) Relict rock glaciers, slope failure deposits, or polygenetic features?
763 A reassessment of some Donegal debris landforms. *Irish Geography* 37, 77-87.
764

765 Wilson P (2009) Rockfall talus slopes and associated talus-foot features in glaciated
766 uplands of Great Britain and Ireland: periglacial, paraglacial or composite landforms?
767 In Knight J, Harrison S (eds) *Periglacial and Paraglacial Processes and*
768 *Environments*. Geological Society, London, Special Publication 320, 133-144.
769

770 Wilson P, Matthews JA, Mourne RW, Linge H, Olsen J. (2020) Interpretation, age
771 and significance of a relict paraglacial and periglacial boulder-dominated landform
772 assemblage in Alnesdalen, Romsdalsalpane, southern Norway. *Geomorphology* 369,
773 107362.
774

775 Winkler S, Lambiel C (2018) Age constraints of rock glaciers in the Southern
776 Alps/New Zealand – exploring their palaeoclimatic potential. *The Holocene* 28, 778-
777 790.
778

779 Zacharda M, Gude M, Růžička V (2007) Thermal regime of three low elevation scree
780 slopes in Central Europe. *Permafrost and Periglacial Processes* 18, 301-308.
781
782
783
784
785
786
787
788
789
790
791
792
793

794 Table 1. InSAR data for seven rock-glacier lobes at Øyberget. Mean velocity refers to
795 groups of points from each rock glacier (June 2015 to September 2019), maximum

796 velocity refers to the point with greatest movement, and temporal coherence indicates
 797 data quality.
 798

Lobe No.	No. of points	Mean velocity (mm/year)	Maximum velocity (mm/year)	Temporal coherence (%)
1	62	-9.5	-19.0	78
1*	48	-12.2	-17.5	79
2	92	-14.5	-24.7	76
2*	57	-17.0	-28.9	70
3	88	-1.2	-22.3	79
3*	52	-22.0	-55.6	72
4	60	-11.3	-30.1	73

799
 800
 801
 802
 803
 804
 805
 806

Table 2. Schmidt-hammer R-values and exposure-age dates with 95% confidence intervals (Ct) for boulder surfaces on rock-glacier lobes (L) and adjacent talus slopes (T) at Øyberget. SD = standard deviation; Cc and Cs are the age-calibration and sampling components of Ct .

Site No.	R-value mean	R-value S.D.	Age (years)	Ct (years)	Cc (years)	Cs (years)	Source
L1	49.28	4.90	10340	±1005	720	705	Matthews et al. (2013)
L2	49.75	6.82	9920	±1385	985	980	..
L3	50.83	8.35	8965	±1680	1180	1195	..
L1*	48.18	6.97	11310	±1305	835	1000	This paper
L2*	52.35	7.20	7620	±1270	850	1030	..
L3*	54.18	7.00	6000	±1220	695	1005	..
T1	50.82	6.81	8975	±1245	775	975	..
T2	58.24	5.39	2400	±980	600	775	..
T3	58.41	5.46	2250	±985	600	785	..

807
 808
 809
 810
 811
 812
 813
 814
 815
 816
 817
 818
 819
 820
 821
 822
 823
 824

Figure captions

825 Fig. 1. (a) Location map with numbered rock-glacier lobes, areas covered by Figs 1b,
826 1c and 2, the location of up-valley control surfaces for SHD, and the sites of ¹⁰Be
827 cosmogenic sampling up-valley and on the summit of Øyberget. (b) Aerial
828 photograph (<https://www.norgebilder.no/>) of the rock glaciers and surroundings. (c)
829 InSAR map of mean velocity for individual points on the rock glaciers and
830 surrounding rock surfaces (<http://insar.ngu.no/>)

831

832 Fig. 2. InSAR map (<http://insar.ngu.no/>) of mean velocity for individual points on
833 rock-glacier lobes 2, 2*, 3 and 3*. Groups of points used for defining representative
834 mean velocities for each lobe are encircled by dashed lines.

835

836 Fig. 3. (a)-(d) Time series of representative mean velocity (groups of points shown on
837 Fig. 2) for rock-glacier lobes 2, 2*, 3 and 3*: InSAR data (<http://insar.ngu.no/>) June to
838 September, 2015–2019.

839

840 Fig. 4. Schmidt-hammer exposure-ages of distal rock-glacier lobes (L1-3), proximal
841 rock-glacier lobes (L1*-3*), and adjacent talus slopes (T1-3). YD = Younger Dryas.
842 Formal subdivisions of the Holocene follow Walker et al. (2018).

843

844 Fig. 5. Schmidt-hammer R-value distributions for distal rock-glacier lobes (L1-3),
845 proximal rock-glacier lobes (L1*-3*), adjacent talus slopes (T1-3), and older and
846 younger control points (blue shading). Vertical lines indicate the mean R-values of the
847 older (green) and younger (red) control points, respectively.

848

849 ****On Fig. 5 T1 (upper right) is labelled as L1.****